Supporting Information

for

Rice Husk-Derived Mn_3O_4/Manganese Silicate/C Nanostructured Composites for High-Performance Hybrid Supercapacitors

Hanmei Jiang[1], Yifu Zhang[*,1,2], Chen Wang[1], Qiushi Wang[1], Changgong Meng[1], John Wang[*,2]

[1]*School of Chemical Engineering, Dalian University of Technology, Dalian 116024, PR China*

[2]*Department of Materials Science and Engineering, National University of Singapore, 117574 Singapore, Singapore*

*E-mail addresses: yfzhang@dlut.edu.cn; msewangj@nus.edu.sg

Figure S1

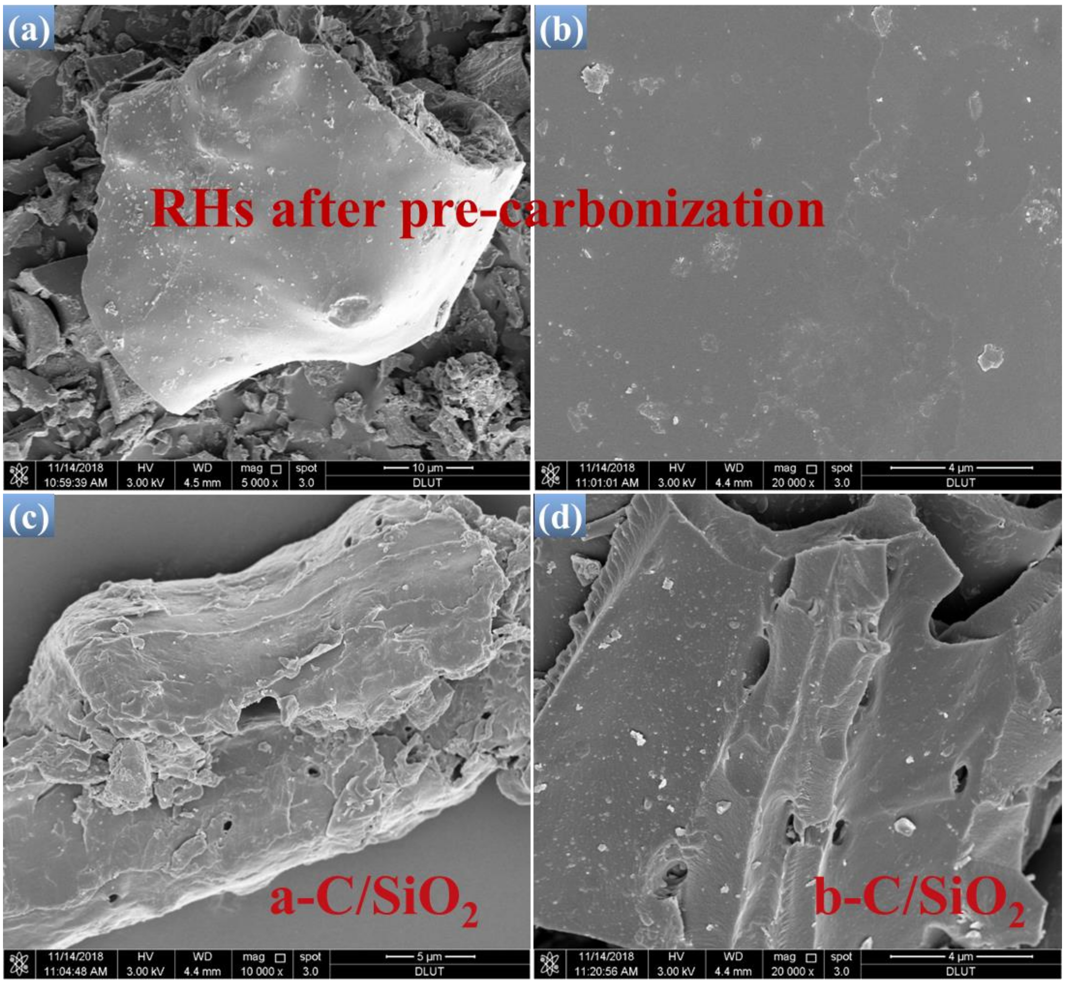

Figure S1. FE-SEM images of (a-b) RHs after pre-carbonization; (c) a-C/SiO_2 and (d) b-C/SiO_2.

Figure S2

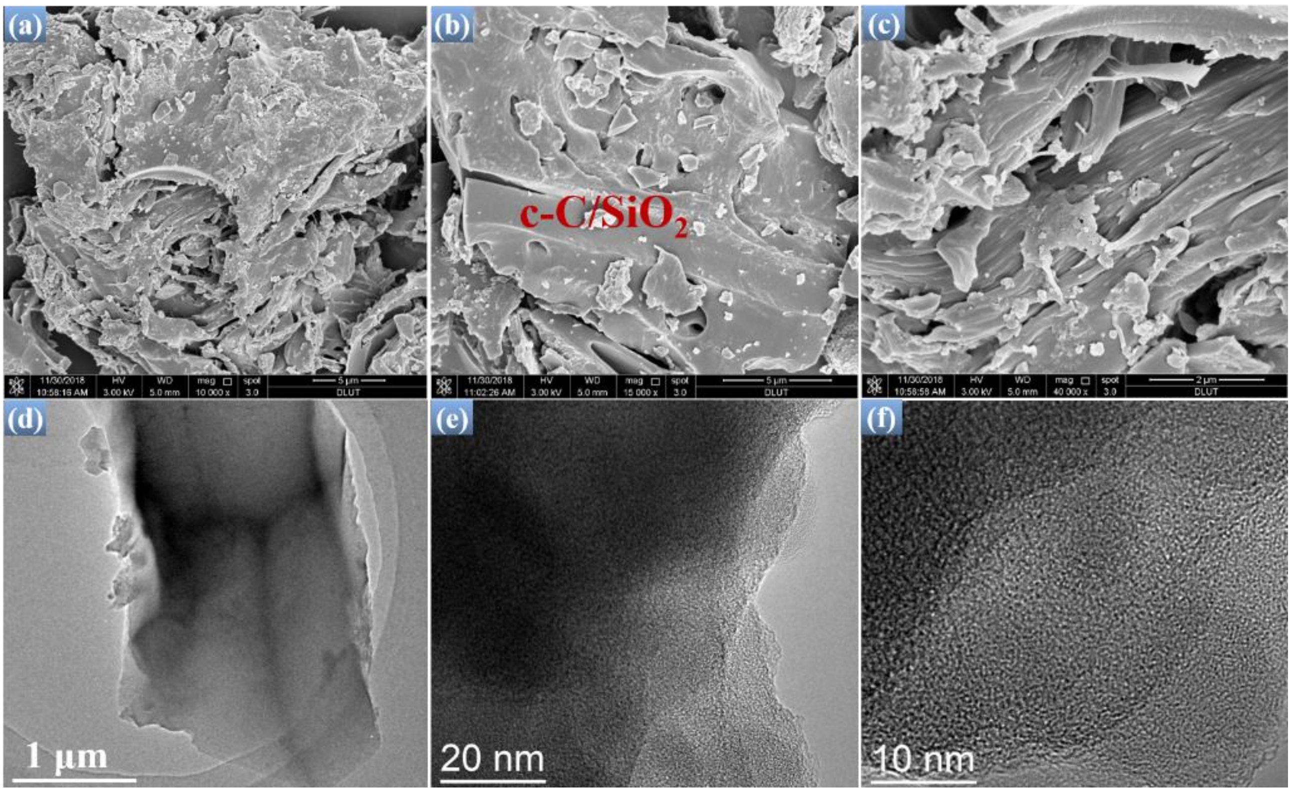

Figure S2. (a-c) FE-SEM images of c-C/SiO_2; (d-f) TEM images of c-C/SiO_2.

Figure S3

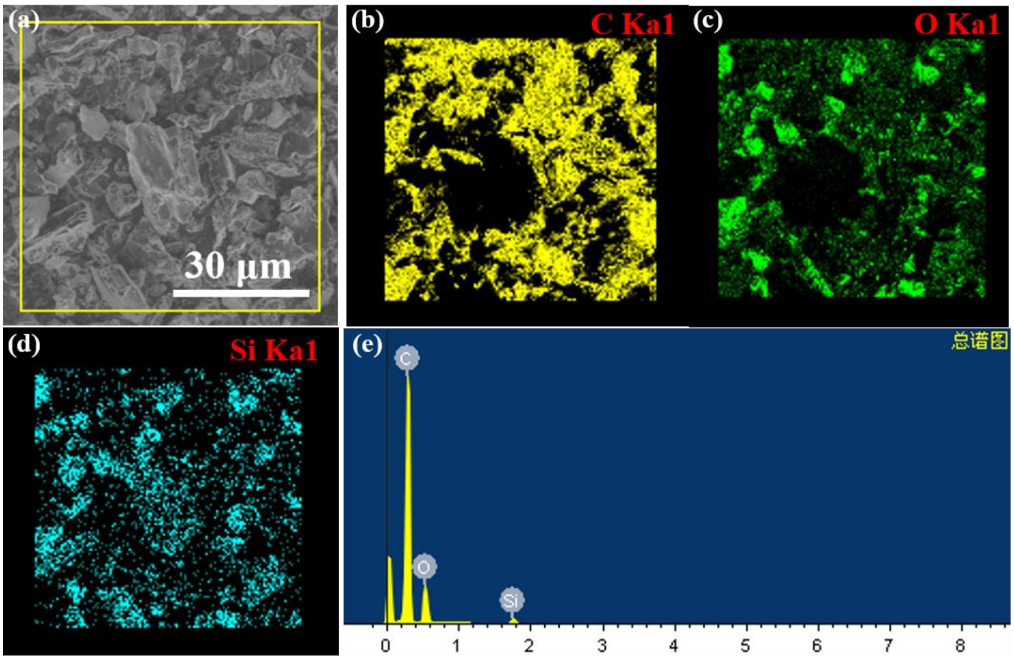

Figure S3. EDS spectrum and elemental mapping images of c-C/SiO_2.

Figure S4

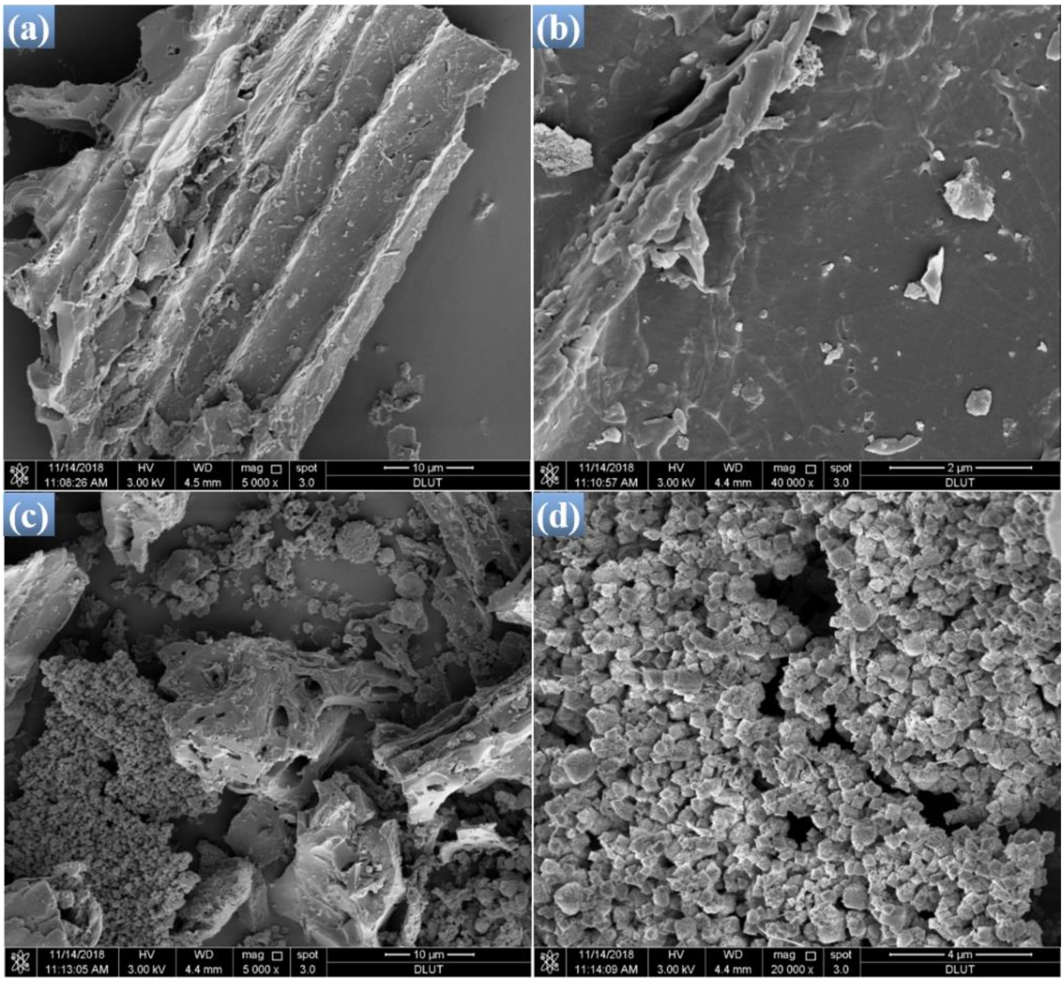

Figure S4. (a-b) FE-SEM images of c-MnSi-0.8; (d-f) FE-SEM images of c-MnSi-3.

Figure S5

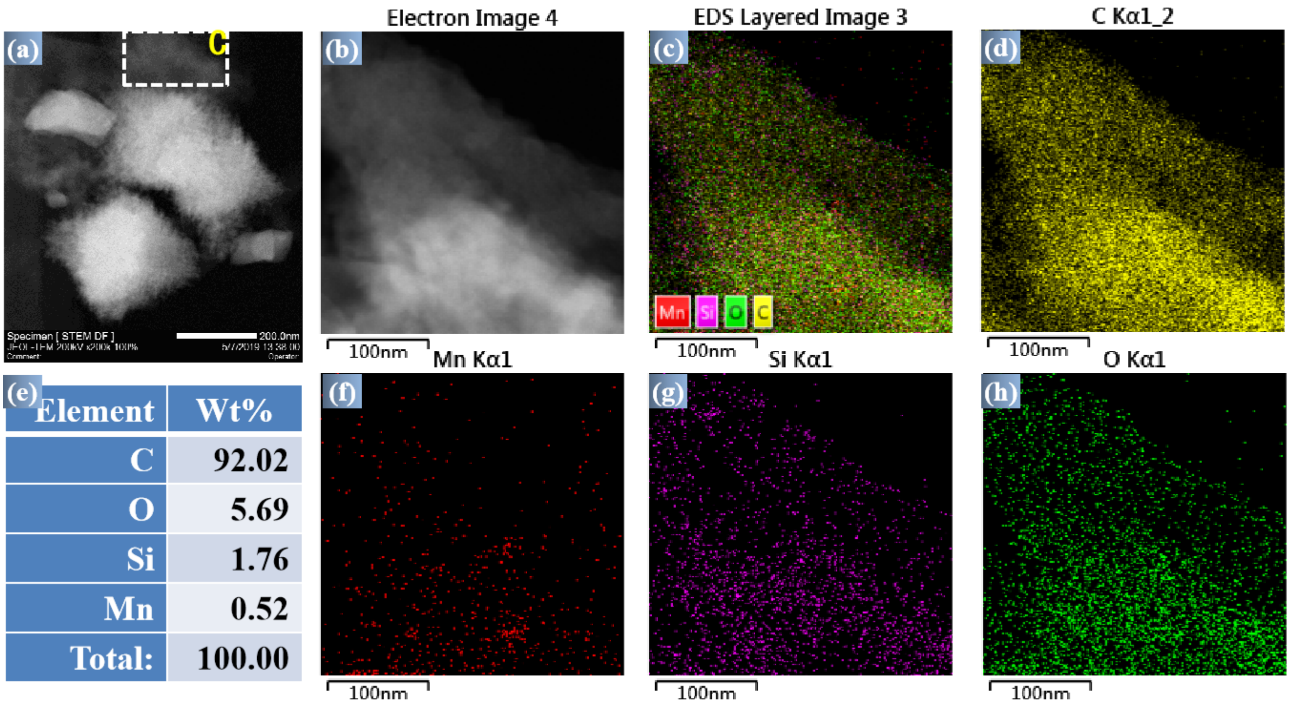

Element	Wt%
C	92.02
O	5.69
Si	1.76
Mn	0.52
Total:	100.00

Figure S5. Corresponding EDS mapping of C basement in c-MnSi-2.

Figure S6

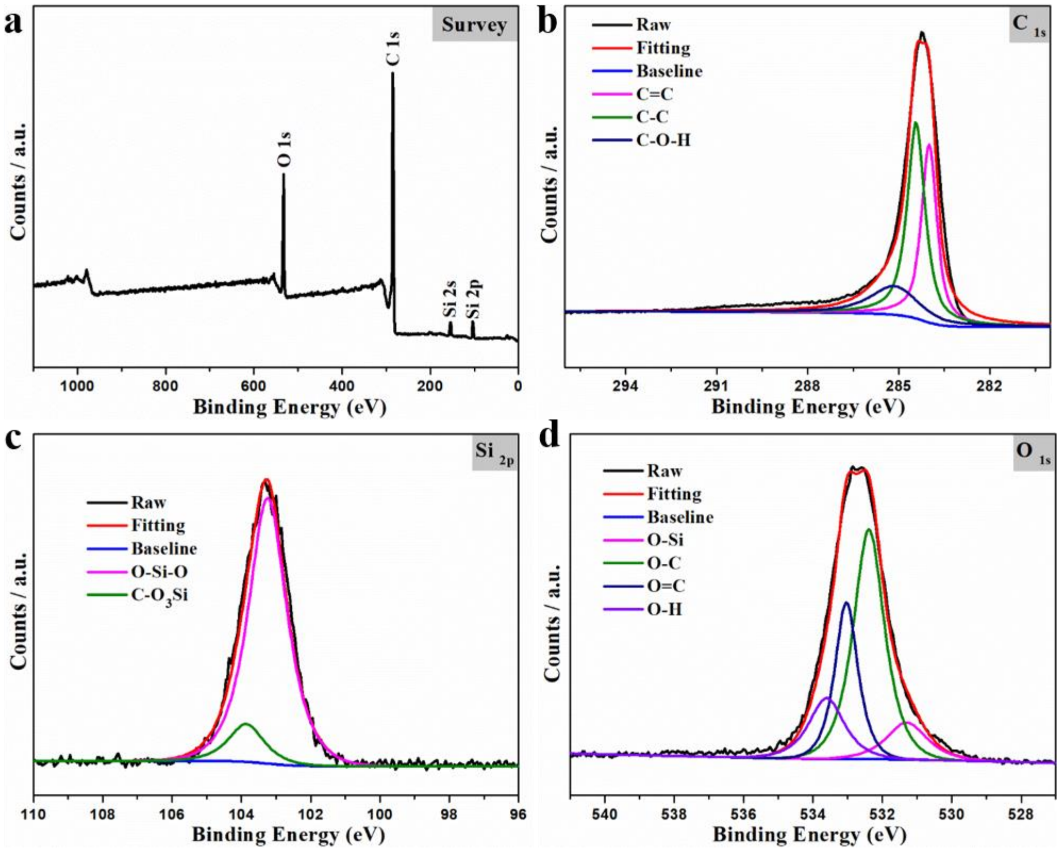

Figure S6. XPS spectra of c-C/SiO_2: (a) Survey XPS spectrum; (b-d) High-resolution spectra of C_{1s}, Si_{2p}, O_{1s}, respectively.

Figure S7

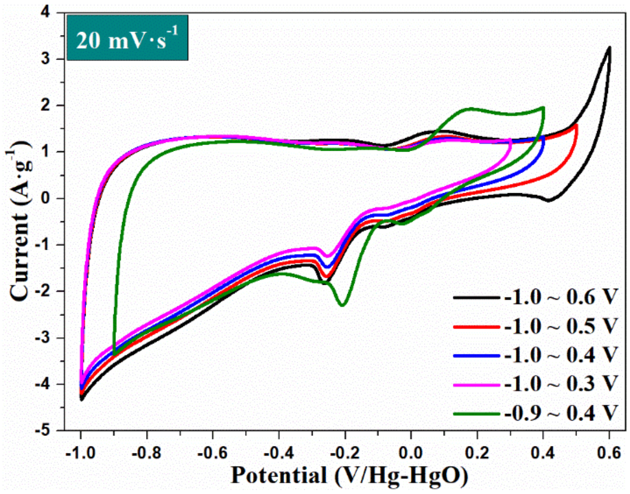

Figure S7. CV curves of c-MnSi-2 at various voltage windows.

Figure S8

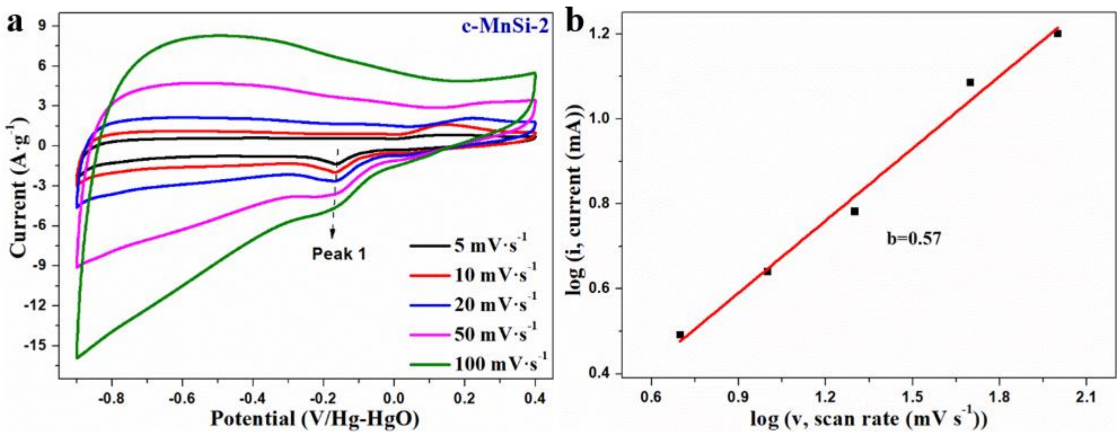

Figure S8. (a) CV curves of c-MnSi-2 and (b) log(i) vs log(v) plots based on peak 1.

Figure S9

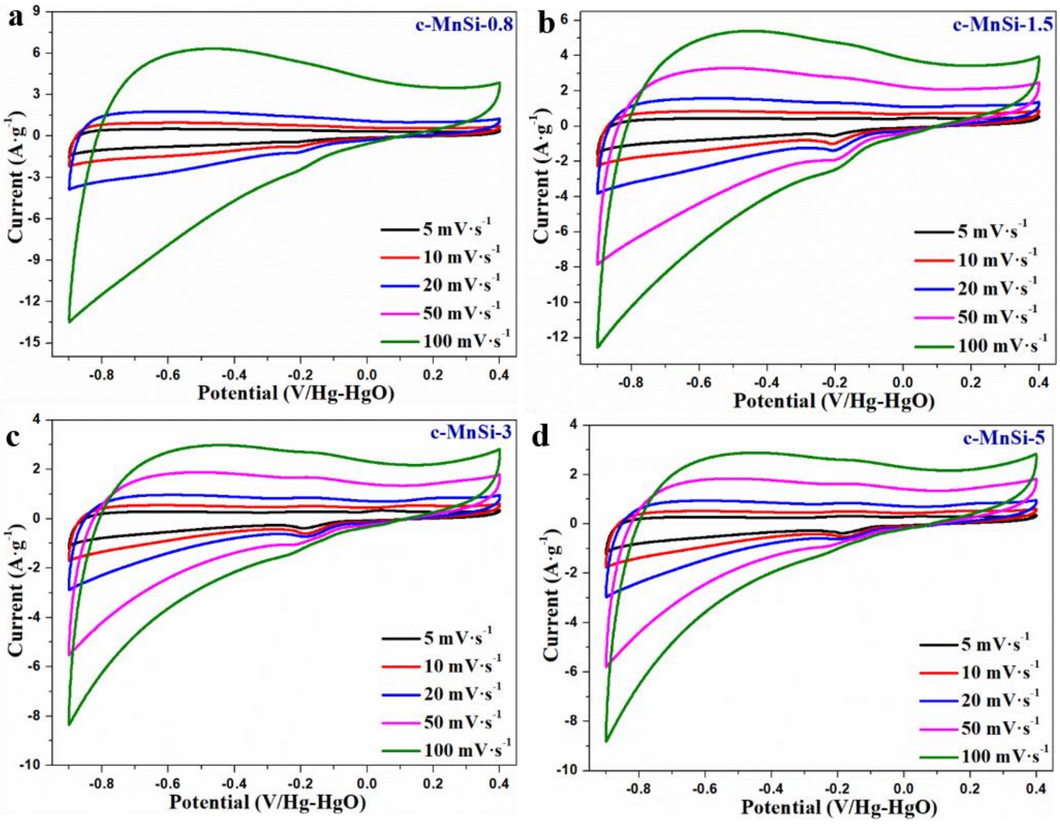

Figure S9. CV curves of the as-prepared samples with various ratios of Mn/Si at different scan rates from 5 mV s^{-1} to 100 mV s^{-1}.

Figure S10

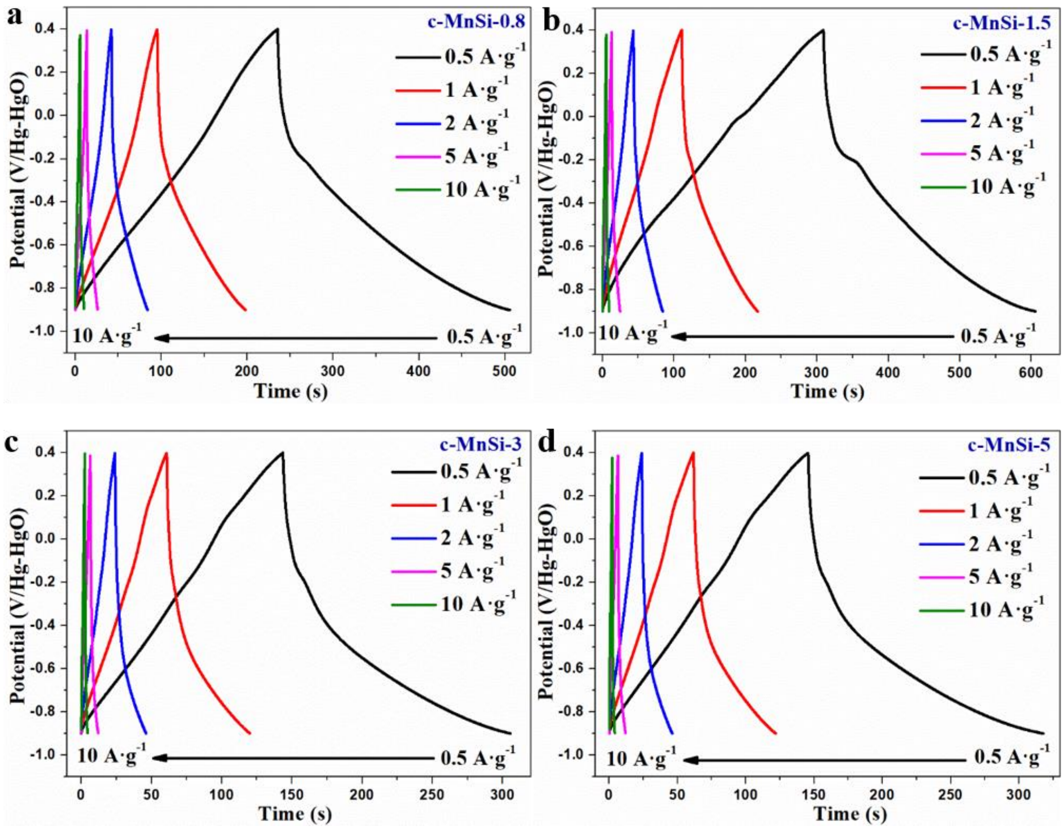

Figure S10. GCD curves of the as-prepared samples with various ratios of Mn/Si at different current densities from 0.5 A g^{-1} to 10 A g^{-1}.

Figure S11

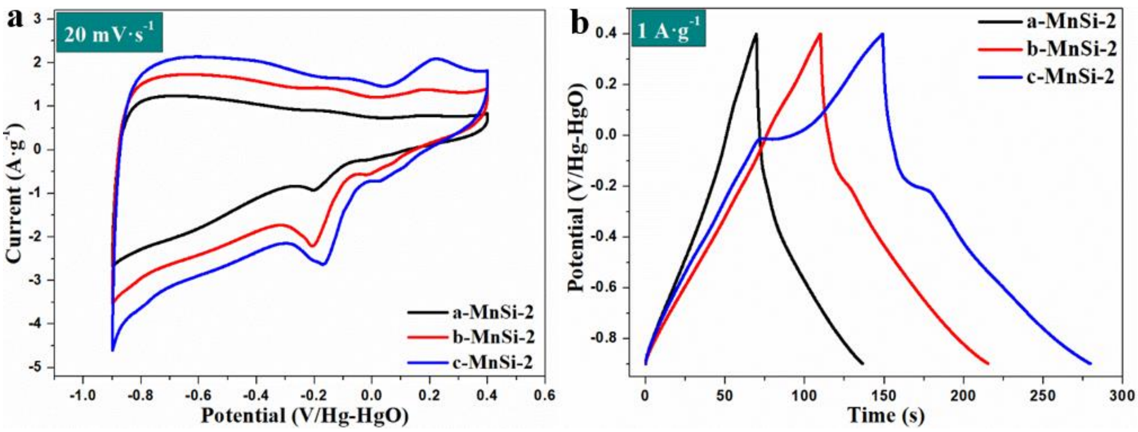

Figure S11. (a) CV curves and (b) GCD curves of as-prepared samples in different active ratios.

Figure S12

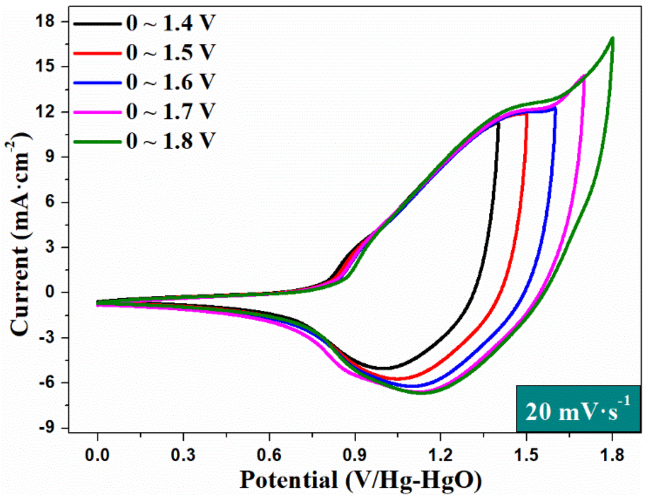

Figure S12. CV curves of c-MnSi-2//$Ni(OH)_2$ HSC on various potential limits.

Figure S13

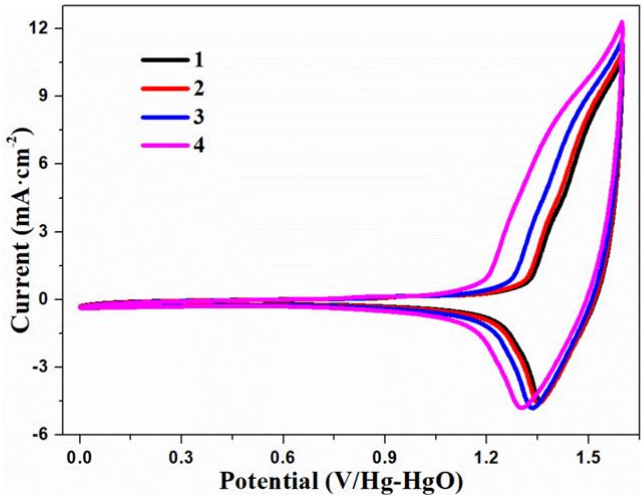

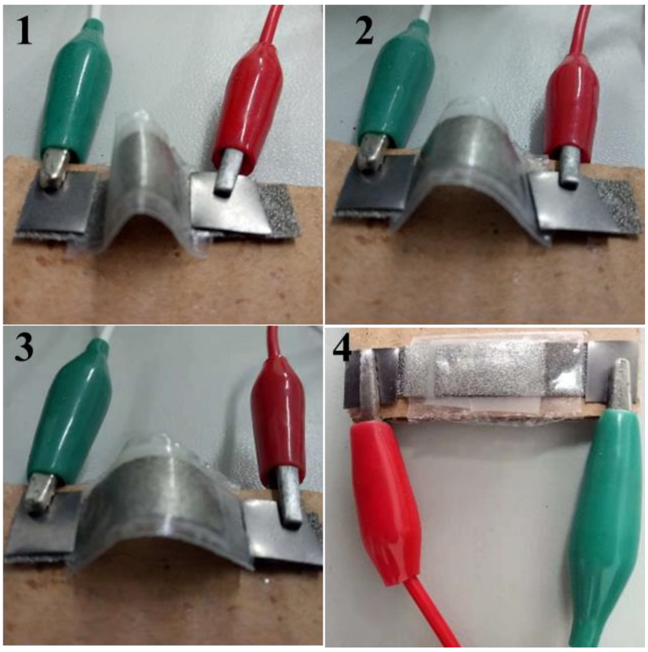

Figure S13. Digital images of c-MnSi-2//$Ni(OH)_2$ ASC bent at various angles and their corresponding CV curves.

Table S1

Table S1. Comparison of the specific capacitance of Mn_3O_4 doped MnSi/C composites and some of other previously reported Mn- and Si- based electrode materials.

Si- or Mn-based materials	Electrolyte	Potential /V	Capacitance	Cycling capability	Ref.
Mesoporous-Li_2MnSiO_4	2 M KOH	0~0.55	120 F g^{-1}, 20 mV·s^{-1}	85.7% after 500	[1]
$Ni_3Si_2O_5(OH)_4$/RGO	2 M KOH	0.2~0.6	178.9 F g^{-1}, 1 A g^{-1}	97.6% after 5000	[2]
NS-C-CoSiO	3 M KOH	−0.05~0.4	1600 F g^{-1}, 1 A g^{-1}	99.1% after 6000	[3]
Mn_3O_4 round shaped nanocrystals	1 M Na_2SO_4	0~0.5	57 F g^{-1}, 2 mV·s^{-1}	81.1% after 1000	[4]
$(Ni, Co)_3Si_2O_5(OH)_4$	1 M KOH	0~0.5	144 F g^{-1}, 1 A g^{-1}	99.3% after 10000	[5]
Manganese silicate drapes	1 M KOH	−0.5~0.4	283 F g^{-1}, 0.5 A g^{-1}	74.7% after 1000	[6]
$Co_3Si_2O_5(OH)_4$	6 M KOH	0~0.5	570 F g^{-1}, 0.7 A g^{-1}	–	[7]
$Co_3(Si_2O_5)_2(OH)_2$	6M KOH	0.1–0.55	237 F g^{-1}, 5.7 mA cm^{-2}	95% after 150	[8]
Mn_3O_4 thin film	1 M Na_2SO_4	−0.1~0.9	314 F g^{-1}, 5 mV·s^{-1}	–	[9]
MnO_2/ZnO	1 M Na_2SO_4	0~0.8	230 mF cm^{-2}, 10 mV·s^{-1}	–	[10]
Cu-doped Mn_3O_4	1 M Na_2SO_4	0~1	134 F g^{-1}, 0.5 A g^{-1}	–	[11]
AMSi/MWCNTs	1 M Na_2SO_4	−0.2~0.8	203 F g^{-1}, 1 A g^{-1}	41% after 1000	[12]
MnO_2/carbon cloth	0.1 M Na_2SO_4	0~0.8	230, 10 mV s^{-1}	98.5% after 3000	[13]
c-MnSi-2	**3 M KOH**	**−0.9~0.4**	**108 F g^{-1}, 1 A g^{-1}[a]**	**82% after 8400**	**This work**

M = mol L^{-1};

[a] The capacitance based on the total mass of the active materials on the two electrodes.

References

1. P. Chaturvedi, A. Kumar, A. Sil and Y. Sharma, *RSC Adv.*, 2015, **5**, 25156-25163.
2. Y. Zhang, W. Zhou, H. Yu, T. Feng, Y. Pu, H. Liu, W. Xiao and L. Tian, *Nanoscale Res. Lett.*, 2017, **12**, 325.
3. X. Li, S. Ding, X. Xiao, J. Shao, J. Wei, H. Pang and Y. Yu, *J. Mater. Chem. A*, 2017, **5**, 12774-12781.
4. D. P. M. D. Shaik, R. Pitcheri, Y. Qiu and O. M. Hussain, *Ceramics International*, 2019, **45**, 2226-2233.
5. Q. Rong, L.-L. Long, X. Zhang, Y.-X. Huang and H.-Q. Yu, *Appl. Energy*, 2015, **153**, 63-69.
6. H.-Y. Wang, Y.-Y. Wang, X. Bai, H. Yang, J.-P. Han, N. Lun, Y.-X. Qi and Y.-J. Bai, *RSC Adv.*, 2016, **6**, 105771-105779.
7. J. Zhao, Y. Zhang, T. Wang, P. Li, C. Wei and H. Pang, *Adv. Mater. Interfaces*, 2014, **2**, 1400377.
8. G.-Q. Zhang, Y.-Q. Zhao, F. Tao and H.-L. Li, *J. Power Sources*, 2006, **161**, 723-729.
9. D. P. Dubal, D. S. Dhawale, R. R. Salunkhe, S. M. Pawar and C. D. Lokhande, *Appl. Surf. Sci.*, 2010, **256**, 4411-4416.
10. W. Zilong, Z. Zhu, J. Qiu and S. Yang, *Journal of Materials Chemistry C*, 2014, **2**, 1331-1336.
11. R. Dong, Q. Ye, L. Kuang, X. Lu, Y. Zhang, X. Zhang, G. Tan, Y. Wen and F. Wang, *ACS Appl. Mater. Interfaces*, 2013, **5**, 9508-9516.
12. Q. Wang, Y. Zhang, S. Jia, Y. Han, J. Xu, F. Li and C. Meng, *Colloid Surf. A-Physicochem. Eng. Asp.*, 2018, **548**, 158-171.
13. Y.-C. Chen, Y.-K. Hsu, Y.-G. Lin, Y.-K. Lin, Y.-Y. Horng, L.-C. Chen and K.-H. Chen, *Electrochimica Acta*, 2011, **56**, 7124-7130.